Available online at www.sciencedirect.com
ScienceDirect
Journal of the European Ceramic Society 28 (2008) 1517–1525
www.elsevier.com/locate/jeurceramsoc

Solid–liquid interactions: The key to microstructural evolution in ceramics

W.E. Lee [a,*], D.D. Jayaseelan [a], S. Zhang [b]

[a] Department of Materials, Imperial College London, South Kensington campus, London SW7 2AZ, UK
[b] Department of Engineering Materials, University of Sheffield, Mappin St., Sheffield S1 3JD, UK

Available online 16 January 2008

Abstract

Five examples from the authors' research are used to illustrate the significance of high temperature solid–liquid interactions in ceramic processing and use. In each system various volumes of liquid form which act as hosts for reactions controlling microstructural evolution. These liquids may have different composition depending on their local environment and they play a dynamic role which can lead to heterogeneous, often non-equilibrium microstructures. The concurrent, often coupled, crystallisation, liquid formation (dissolution and melting) and volatilisation processes are highly complex but of great practical importance.

Keywords: Refractories; Mullite; Glass ceramics; Mineralization; Microstructures

1. Introduction

An important aspect of microstructural evolution, often overlooked, is the impact of liquid formation and its interaction with solid phases during high temperature firing and use of complex multiphase ceramic systems.[1] Solid–liquid interactions are poorly understood even in the simplest systems and the current state-of-the-art in atomic scale modeling even at room temperature involves interfaces between pure amorphous silica and pure water.[2] The additional complexity of varying liquid composition, pH, temperature and viscosity as well as solid composition, crystallinity, microstructure, temperature, defect content and atmosphere has been little considered. We are a long way from a full understanding, across all length (and time) scales of solid–liquid interactions in any real ceramic systems. Such systems are of immense importance and include replacement bone/body fluid, refractories/slag, high-level radwaste glass/repository water, and liquid phase and viscous composite sintered commercial ceramics. This paper will summarise recent research in the authors group looking at liquid formation and solid–liquid interactions in a number of ceramic systems. Specific examples of the impact of liquid composition and viscosity will demonstrate that these systems are generally far from thermodynamic equilibrium and that the liquids formed are often significantly heterogeneous varying in composition (and hence properties) with location in the microstructure. The importance of this local liquid on microstructural evolution will be discussed.

2. Background

The vast majority of commercial ceramics are made via processes which involve complete system melting such as fused refractories, glasses and glass ceramics, high (up to 60 vol%) liquid formation such as viscous composite sintered whitewares and structural clay products, or significant (up to 20 vol%) liquid formation such as liquid phase sintered structural and electroceramics. However, studies of the liquids formed in them are limited. Formation of liquids from interaction of reactant powders on firing a green body, their change in composition/viscosity with time/temperature and atmosphere, and their variability with location are all poorly understood. Even at room temperature, interaction of ceramic powders with water and solvents during green state processing, of bioceramics with body fluids and many other cases demonstrate our lack of knowledge even when the complexity of high temperature is not present.

Any chemical reaction between a solid body and a liquid involves reactant contact enabling the reaction to take place and product transport to allow it to proceed. Wetting of solid

* Corresponding author. Tel.: +44 20 7594 6733; fax: +44 20 7594 6736.
E-mail address: w.e.lee@imperial.ac.uk (W.E. Lee).

0955-2219/$ – see front matter © 2007 Elsevier Ltd. All rights reserved.
doi:10.1016/j.jeurceramsoc.2007.12.010

ceramics by liquids at the simple macroscopic level is defined by the value of the contact and dihedral angles determined by the interface energies[1] but the complexities introduced in real heterogeneous systems with varying composition, rugosity and temperature are only now becoming better understood.[3] Full understanding of the dynamic change in composition and viscosity as a liquid reacts with different phases in a multiphase system and its penetration around the system requires more than the Poiseuille and Stokes–Einstein relations[4] and the ability to model at the atomistic scale in real systems is still lacking. We can model the thermodynamic equilibrium in such systems[5,6] and perform detailed electron microscopy of interface glass compositions[7] (assuming they are derived from high temperature liquid) but we are as yet a long way from being able to model what has happened at the atomic level in systems for which we have detailed *post mortem* microstructural analysis. The holy grail of being able to predict what will happen in systems without the need to recourse to empirical studies is still for the future.

Microstructural development in ceramics has traditionally been examined using simple interrupted heat treatment and quench studies with the microstructures being characterised *post mortem* at room temperature using, e.g. XRD, optical microscopy, TEM, SEM and NMR, e.g. ref. [8]. Dynamic, *in situ*, solid–liquid interaction studies have been, and are being, attempted but particularly at high temperature are empirically difficult and are hard to align with practical conditions of interest. Development of suitable stages in appropriate characterisation instrumentation (optical microscopes, SEMs, ESEMs, TEMs, STMs) has improved the situation but interpretation of the data can be complicated.[9,10]

3. Corrosion of refractories by silicate slags

The attack of refractory furnace linings by molten liquids including silicate slags is of great commercial interest to high volume materials (e.g. steel, glass and cement) producers. As a result many simple empirical tests, including static finger and crucible tests and more dynamic rotary slag tests,[4] have been developed to try and simulate furnace conditions enabling better lining materials to be developed. *Post mortem* examinations of corroded and failed furnace linings, e.g. ref. [11] often reveal formation of low melting phases and eutectics responsible for the failure but also highlight the importance of location in the furnace and the local equilibrium specific to a particular region. Direct (congruent or homogeneous) attack is controlled by the reaction rate at the slag–refractory interface or the rate of diffusive transport of species to it through the slag leading to *active* corrosion. Indirect (incongruent or heterogeneous) attack is controlled by diffusive transport through the slag or through a new solid phase, which forms at the original slag–refractory interface. This may lead to *passive* corrosion and extended lining lifetimes. Examples of direct and indirect attack in a range of refractory/slag systems[4,12–14] highlight the critical influence of the composition and hence viscosity of the local liquid slag adjacent the solid refractory. Penetration and corrosion can be controlled[15,16] either through the local slag composition via the refractory[17] or the bulk slag or by microstructural control of the refractory by, e.g. internal generation of dense layers or external deposition/generation of passive coatings, so-called *in situ* refractories.[18] The presence of fluidising cations (such as alkalis, Ca or Fe) in a liquid silicate slag can encourage solid oxide dissolution and lead to extensive penetration and eventual lining failure. Fig. 1 shows schematically the interaction of penetrating slag with the microstructure of a typical refractory consisting of a fine (often nanoscale) multiphase bond system holding together large (up to mm) aggregates or grains. The silicate liquid slag is enriched in more rapidly moving (and fluidising) cations at the solid–liquid interface.

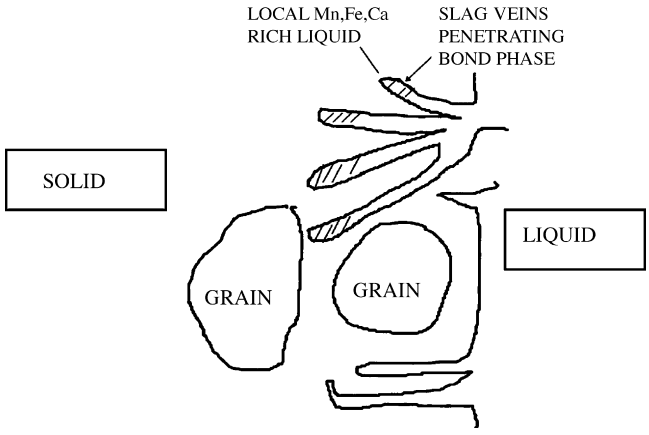

Fig. 1. The variation in slag composition, being richer in fluidising cations near the solid, drives the process. Adapted from ref. 4.

Clearly, the solid–liquid interaction in this situation will be complex involving initial fine solid dissolution, and precipitation of solids both at temperature and on cooling. However, it is the ability of solid aggregate materials such as MgO, spinels, mullite, forsterite and Al_2O_3 to take fluidising cations into their crystal structures at temperature, leaving behind a viscous and less penetrative liquid or to react with them to form protective layers, that is a key aspect of the refractories good resistance to slag attack. It is the heterogeneity of the liquids composition gradient which enables this process to occur. Fig. 2 shows protective layers of calcium hexaluminate (CA_6) and Fe-containing hercynitic spinel formed around a white fused alumina (WFA) grain after corrosion in a silicate slag for 1 h at 1450 °C. In this example the spinel being formed by reaction of the solid alumina with MgO-rich slag becomes more iron-rich as it grows into the adjacent slag, again denuding the slag of fluidising cations.

It is the composition of the liquid directly adjacent the solid, the local liquid, that is important to the process protecting the refractory from attack.

4. Mullite formation and morphology in clay-derived ceramics

High-volume, inexpensive and clay-derived ceramics are used extensively as whitewares, structural clay products and refractories. They are usually triaxial mixtures of clay, flux and filler with a complex microstructural evolution on firing.[19–23] Mullite is the key phase in these vitreous ceramics as it is

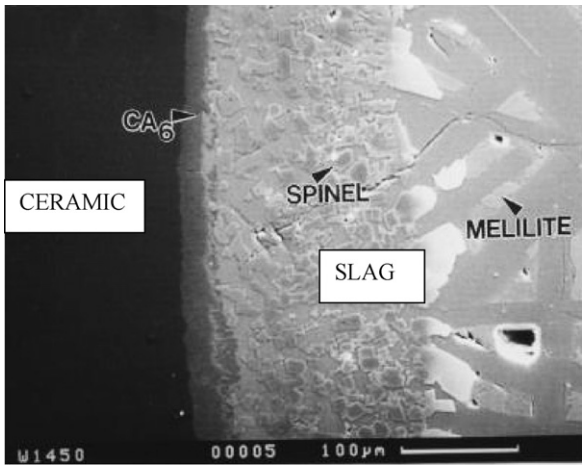

Fig. 2. Backscattered electron SEM image of WFA grain protecting itself via formation of CA_6 and spinel layers. Note the spinel has brighter contrast due to high Fe content deeper in the slag. Adapted from ref. 13.

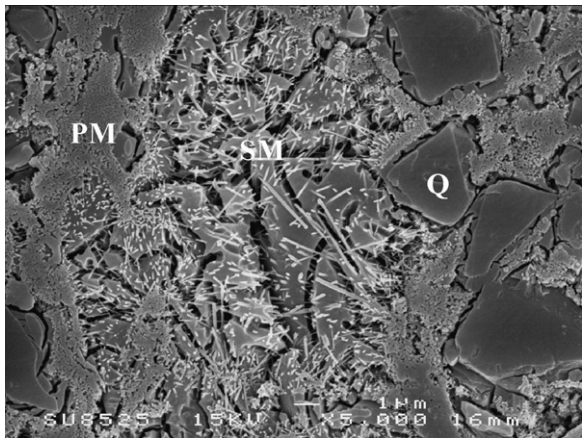

Fig. 3. SEM image of model porcelain fired 3 h at 1075 °C containing 50 wt% clay, 25% nepheline syenite and 25% quartz revealing quartz filler (Q), cuboidal primary mullite (PM) and acicular secondary mullite (SM). Figure courtesy GP Souza.

believed to affect the mechanical properties of the bodies containing it via its interlocking, acicular morphology and the stress generated in the glassy matrix due to the expansile nature of its formation mechanism. Two forms of mullite predominate in vitreous ceramics. *Primary* mullite, which is first to form on firing from decomposition of "pure" clay and has cuboidal or scaly morphology. *Secondary* mullite, which is the second to form from decomposition of the flux and its reaction with the clay, and which has a granular or acicular morphology.

The interactions between the various starting materials in model bone china, porcelain and stoneware systems have been interpreted from interrupted quench studies as recently reviewed by Lee et al.[24] These reveal the importance of mixing of the raw materials to the later evolution on firing[25] since the extent of mixing controls the location of the first liquid to form from the lowest melting components and the surrounding phases which then control the liquids changing composition as it reacts with them. A silicate liquid high in alkalis (in a feldspar-rich flux region) will be highly fluid leading to formation of acicular secondary mullite whereas regions containing only pure clay will be more silica-rich and viscous forming smaller, cuboidal primary mullite. The formation of different mullite morphologies in different regions of the microstructure highlights the heterogeneity of the liquids from which they grow. The liquid composition clearly varies with location and it is the local liquid composition which controls the phase formation and morphology.

The composition and hence viscosity of the silicate liquid, which is crucial to the mullite morphology which forms, can be controlled not only by the raw materials used and the extent of mixing but also by atmosphere-induced changes to the liquid composition in Fe-containing systems.[26] The silicate liquid is more fluid in oxidising atmosphere due to removal of fluidising Fe as metal under reducing atmosphere. The mullite formed from the resulting silica-rich, viscous liquid is smaller and less acicular. Use of waste soda–lime–silica (SLS) glass as partial replacement of the mined feldspar flux has a large influence on the silicate liquid composition and the microstructures formed.[22,23] Use of SLS glass leads to formation of additional phases including wollastonite, plagioclase and sodium silicates and less mullite forms due to the decreased Al_2O_3 content on replacing Na feldspar with SLS glass (Fig. 3).

Even in pure clay systems the composition and viscosity of the liquid formed on firing is complex.[27,28] Since clays are natural minerals they contain various levels of impurities including, significant for mullite formation, alkalis and Fe-containing compounds. Furthermore, different types of clay contain different species especially alkalis within their crystal structures which on decomposition of the clay lead to more fluid silicate liquids. The interactions between model binary (e.g. flux–clay, clay–filler), ternary (e.g. clay–flux–filler) and quaternary (e.g. clay–feldspar–SLS glass–filler) systems on firing have recently been examined by Tarvornpanich et al.[29,30] They found complex multidimensional concurrent liquid formation and crystallisation processes determined the composition/viscosity of the high temperature liquid. The local liquid compositions were variable, more so in the higher component systems. Fig. 4 shows schematically the heterogeneous nature of the microstructures in such systems and highlights that the liquid matrix at temperature consists of a number of different composition local liquids.

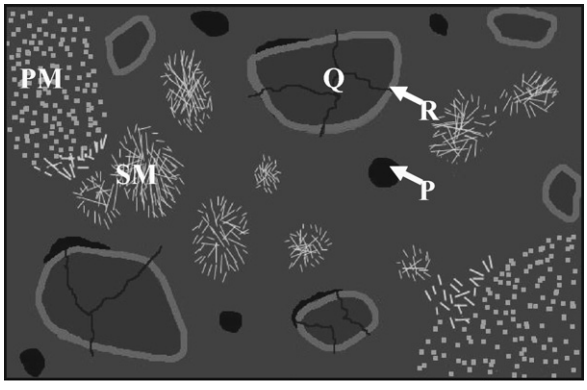

Fig. 4. Schematic diagram of a typical porcelain microstructure showing primary mullite (PM) in an essentially pure aluminosilicate liquid, cracked quartz filler (Q) surrounded by a predominantly silica solution rim liquid (R), matrix pores (P) and secondary mullite (SM) in an alkali-rich aluminosilicate liquid.

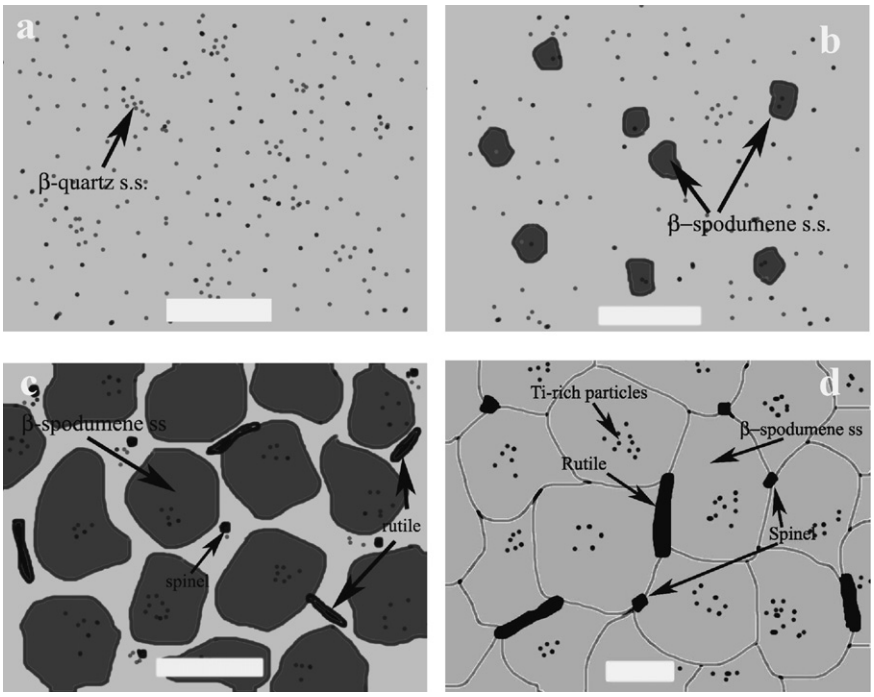

Fig. 5. Schematic of phase evolution in model CorningWare glass. (a) Precipitation of β-quartz s.s., (b) formation of β-spodumene s.s., (c) growth of β-spodumene s.s. alongside rutile rods and (d) impingement of growth of β-spodumene s.s. with minor rutile and cuboidal spinel (bars = 0.5 μm). From ref. 40.

A further complication in vitreous systems is mullites range of stoichiometry, typically from 3:2 to 2:1 Al_2O_3:SiO_2. The stoichiometry of mullite embedded in complex aluminosilicate liquids is contentious and difficult to measure. Conventionally-derived mullite is stable 3:2 formed by solid state reaction and acicular 2:1 formed from the melt in the presence of liquid glassy phase as expected from the commonly accepted phase diagram of Aksay and Pask.[31] It is worth noting that mullites observed in vitreous systems are likely to be far from equilibrium so that interpretations based on phase diagrams are unlikely to apply. We believe that there is a spread of mullite compositions in vitreous systems across the 2:1 to 3:2 range in vitreous systems with the exact composition being dependent to large extent on the local liquids composition particularly the availability of Al_2O_3.[24]

5. Crystal formation in silicate glass ceramics

Interrupted quench studies and detailed *post mortem* microstructural characterisation have been used for many years in an attempt to understand the crystallisation mechanisms of complex, multiphase, silicate glass ceramics, e.g. refs. [32–36]. The mechanism of microstructure formation via crystallisation from glasses makes the microstructures of glass ceramics very different from the simple grain structures of most powder-derived polycrystalline ceramics. Beall[37,38] summarised the main groupings of the final glass–ceramic microstructures into, e.g. dendritic, ultra-fine grained (what might now be termed nanocrystalline), cellular membrane, relict, house of cards, coast and island, acicular interlocking, and lamellar twinned. However, the evolution of the microstructures from the glass to the final glass–ceramic microstructure has been given less attention. In particular, the concept of crystallisation hierarchies[35,39] which considers that crystals form, sometimes simultaneously sometimes sequentially, at different length scales on crystallising glass ceramics is only just beginning to be recognised. Recent studies of commercial silicate glass ceramics and model systems[39,40] revealed that phase separation in the glass (viscous liquid) during the early stages of heat treatment initiated crystallisation in both fluormica- (Macor) and cordierite- (Corning Code 9606) based systems. This led to at least two differing composition glasses from which crystallisation could proceed via formation of several phases at different scales of size, the first phases to form being those containing the most rapidly diffusing species. In Macor-type compositions this was by simultaneous nucleation of ~0.3 μm chondrodite and 3–4 μm fluorophlogopite laths while in Corning 9606-type compositions it was by simultaneous nucleation of μ-cordierite nanocrystals and ~0.2 μm $MgAl_2Ti_3O_{10}$ rosettes.

Fig. 5 illustrates the crystallisation of a model CorningWare, lithium aluminosilicate glass ceramic composition showing initial nucleation of a β-quartz solid solution composition at the nanoscale, a separate later crystallisation of a β-spodumene solid solution phase before growth and final evolution to a fully crystallised β-spodumene solid solution with minor rutile, spinel and Ti-rich phases.[40]

Once again this shows the importance of the local viscous liquid (glass) composition on phase formation and illustrates that the phases that form depend on the local environment. Glass ceramics do however highlight that once one (or more) phases have crystallised, the composition of the remaining liquid is denuded of the crystal-forming elements so that another new phase may evolve. Many commercial glass ceramics are

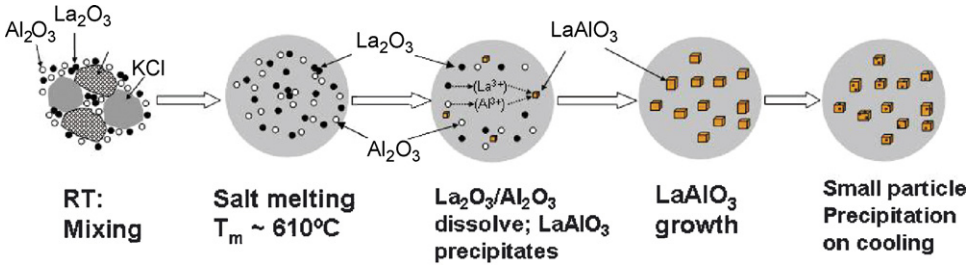

Fig. 6. Schematic of solution-precipitation mechanism of MSS synthesis of $LaAlO_3$.

observed to contain small pockets of almost pure silica glass in their microstructures; the final phase from which crystallisation is almost impossible. A common observation in glass ceramics is that metastable crystals form that are later consumed by more stable crystals. Their role and the importance of the change of glass composition during coupled crystallisation of several phases is worthy of further study.

6. Mechanisms of ceramic powder formation from molten salt precursors

Synthesis of ceramic powders with varying morphologies from low melting salt systems is of current interest due to the flexibility of the processing route and its ability to form refractory powders at low temperatures.[41–46] Generally, two reaction sequences are considered in molten salt synthesis (MSS): solution-precipitation and template formation. In the solution-precipitation route, the reactants dissolve in the molten salt, followed by formation of the product in the molten salt medium and finally precipitation of the product above its solubility limit. The mechanism is illustrated schematically in Fig. 6 for $LaAlO_3$ powder production from La_2O_3, Al_2O_3 starting oxides and a range of salts.[44]

Both starting oxides dissolve in the molten salt which (for a KCl-KF eutectic) begins to melt at 610 °C. Cuboidal $LaAlO_3$ precipitates from the liquid once the salt is oversaturated with it and grows. While the $LaAlO_3$ is typically cuboidal in shape arising from its rhombohedral crystal habit, its size can be controlled via the salt/oxide ratio or temperature being larger at higher temperature and decreasing with increasing salt/oxide ratio presumably because the liquid is more fluid, more able to form nuclei but less able to grow since it contains proportionally less of the oxides needed to form the aluminate. Small non-cuboidal $LaAlO_3$ particles observed precipitating on the large cuboidal crystals presumably form on cooling as the liquid becomes oversaturated with the oxides as the temperature lowers (Fig. 7).

In the template formation mechanism, one of the reactants dissolves in the molten salt and the dissolving component is transported to the outer surface of the other reactant and the product is formed on the latter's undissolved surface. Template growth has been used to synthesise $MgAl_2O_4$ spinel on Al_2O_3 platelets in $MgSO_4$ salt[41] and later K_2SO_4 salt as well as MCl chlorides where M = Li, Na and K.[45] Fig. 8 shows spinel platelets formed on alumina templates using MgO as the MgO source in K_2SO_4 salt after 3 h at 1150 °C.

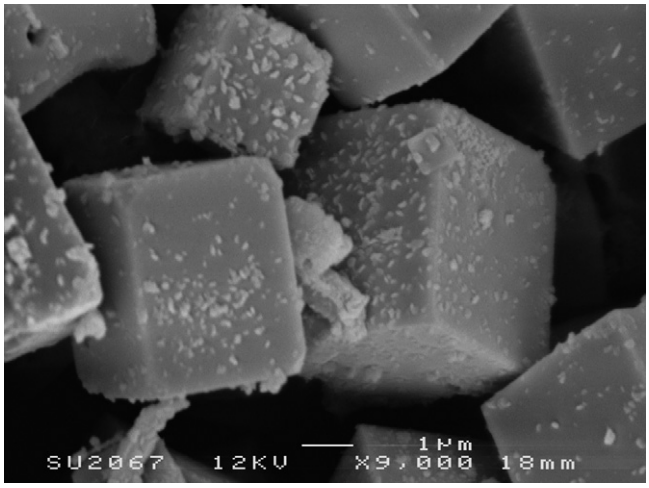

Fig. 7. Cuboidal $LaAlO_3$ particles synthesized using 3:1 salt/oxide weight ratio heated 3 h at 700 °C. Note the small irregular $LaAlO_3$ particles decorating the cuboids. Adapted from ref. 43.

Note the roughness of the platelet surfaces. High-resolution SEM studies of similar platelets[46] reveal varying size spinel crystallites growing on the polycrystalline spinel platelets. The difference in size of the crystalline spinel particles appearing on the platelets can be explained by the viscosity of the molten reactants. For example, when MgO dissolves in the salt, its fluidity is lower than when $Mg(NO_3)_2$ dissolves in it. With highly fluid molten liquid the wettability is higher and the reaction is quicker

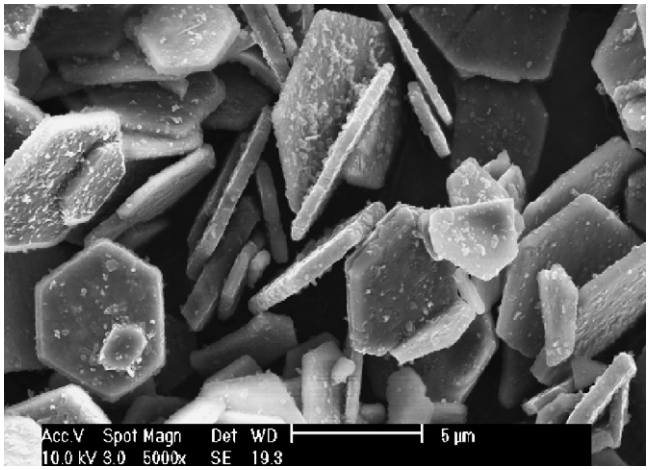

Fig. 8. Spinel platelets synthesised using MgO as the MgO source in K_2SO_4 salt.

leading to nanocrystalline particles because more nuclei form at an early stage but their growth is constrained due to limited time. In a viscous liquid fewer nuclei form as mass transport is restricted. Hence the nuclei grow to larger size giving the platelets a more roughened appearance.

Again the importance of the solid–liquid interactions and especially the composition and viscosity of the local liquid adjacent to the reacting solid is highlighted.

7. Mineralisation mechanism of spinel formation from Al_2O_3 and MgO using B-containing additives

Mg aluminate spinel is used in the bond systems of many refractories, formed by pre-reaction of MgO and Al_2O_3, by *in situ* reaction on firing or in service.[47] Spinel formation is known to occur at lower temperature in the presence of B-containing compounds but their use needs careful control since B-compounds also lower the refractoriness of the spinel and the refractory system. This ability to lower the temperature of formation of compounds is termed mineralisation. Mineralisers are compounds that are added in small amounts to a reaction mixture to assist formation and/or crystallisation of other compounds on firing with or without incorporating themselves in the product crystal structures. They function in various ways by, e.g. lowering the phase formation temperature and increasing phase stability, accelerating the rate of a solid state reaction, and altering the viscosity and surface tension of participating liquids affecting crystal growth and morphology. Examples include alkalis mineralising the quartz to cristobalite transformation and iron oxides the growth of mullite crystals.

Recent interrupted quench studies[48,49] examined the reaction of MgO and Al_2O_3 powders in the presence of 0–10 wt% B_2O_3, $Li_2B_4O_7$ and $Na_2B_4O_7$ using a range of characterisation techniques to determine the mechanisms of mineralisation. B_2O_3 was observed to mineralise spinel formation from stoichiometric (1:1 mole ratio) calcined magnesia and alumina.[47] After 3 h at 1100 °C, XRD shows the mineralization effect of B_2O_3 is limited to 1.5 wt% additions with higher B_2O_3 contents leading to $Mg_3B_2O_6$ formation and reduced spinel content. ^{11}B NMR, EPMA, SEM, TEM and XRD reveal formation of a boron-containing liquid. EDS in the TEM and EPMA of the glassy phases formed from solidification of the liquid reveal that initially it is Mg borate, later becoming a magnesia-modified boroaluminate composition, suggesting dissolution–precipitation as opposed to templated growth as the mechanism of this liquid phase mediated mineralisation shown schematically in Fig. 9. After 3 h at 1000 °C in a stoichiometric Al_2O_3–MgO mix containing 1.5 wt% B_2O_3 the fine submicron MgO is dissolving in B_2O_3 forming Mg borate liquid. By 1100 °C this liquid has also started to dissolve Al_2O_3 forming Mg boroaluminate liquid. Both oxides dissolve (in the liquid) but at different rates encouraging mass transport and mediating the spinel-forming reaction.

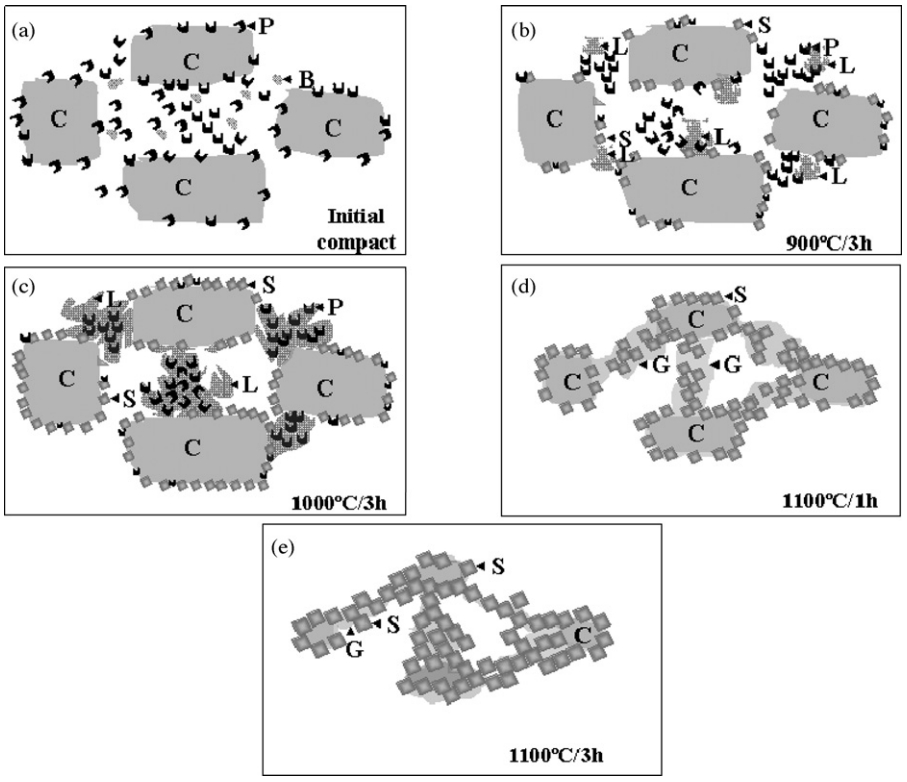

Fig. 9. Schematic of mineralisation of spinel formation by B_2O_3. (a) Fine magnesia and B_2O_3 dispersed among large alumina grains, (b) boron oxide melts (melting temperature 450 °C) and spinel formation begins on alumina surfaces, (c) liquid volume increases with MgO dissolution and further spinel forms, (d) B and Mg-containing liquid dissolves alumina, wetting all grains and precipitating spinel, (e) corundum shrinks, spinel grows forming a network, S = spinel, B = boron oxide, P = periclase, C = corundum, L = Mg borate liquid and G = Mg boroaluminate liquid.

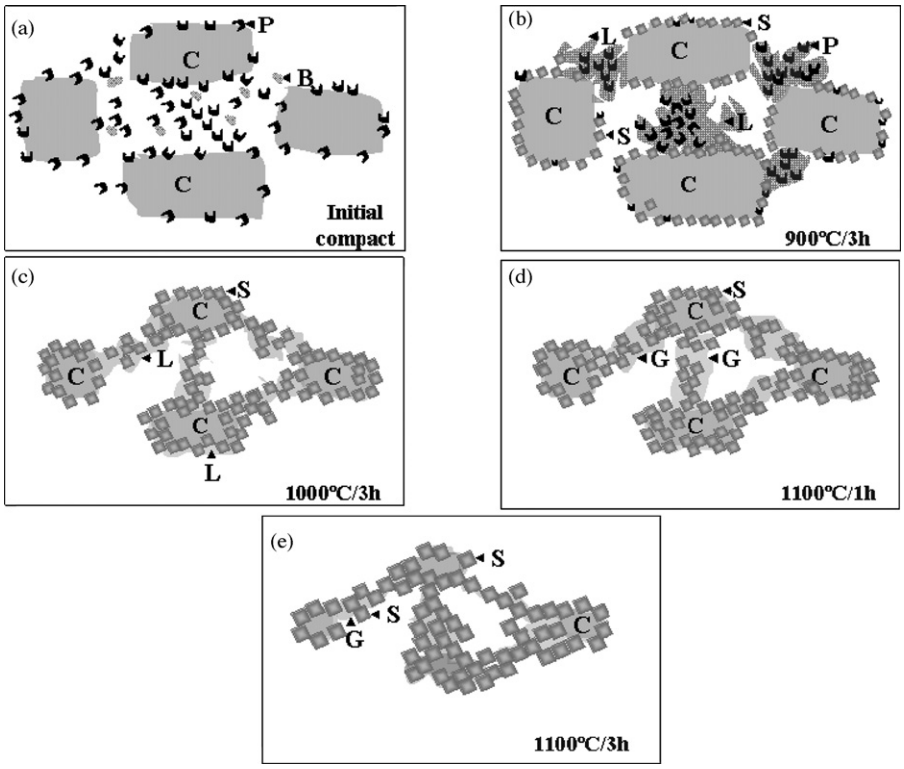

Fig. 10. Schematic of mineralisation of spinel by 1.5 wt% $Na_2B_4O_7$: (a) fine magnesia and $Na_2B_4O_7$ dispersed among large alumina grains, (b) $Na_2B_4O_7$ melts at 751 °C dissolving magnesia by 900 °C forming Mg,Na borate liquid and spinel formation begins on alumina, (c) liquid volume increases with dissolution of more magnesia (leaving no unreacted periclase), spinel increases, (d) corundum level reduces, spinel grows, (e) small corundum cores remain. S = spinel, B = $Na_2B_4O_7$, P = periclase, C = corundum, L = Mg, Na borate liquid and G = Mg, Na boroaluminate liquid.

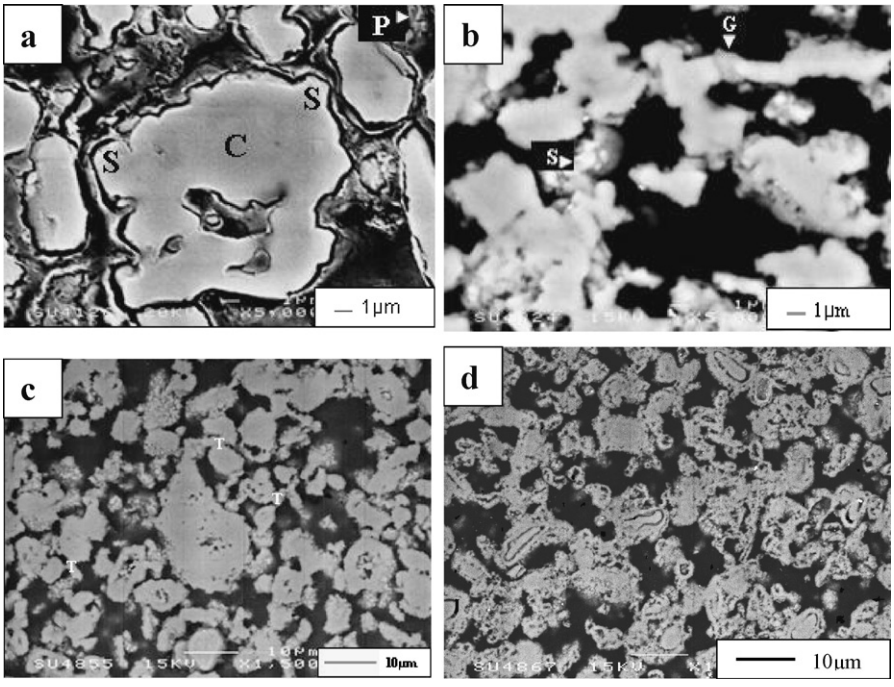

Fig. 11. Comparison of spinel morphologies after 3 h at 1100 °C with (a) no mineraliser, (b) 1.5 wt% B_2O_3, (c) $Li_2B_4O_7$ and (d) $Na_2B_4O_7$. S = spinel, C = corundum, P = periclase, G = glass, T = tuber-like.

Similarly, $Li_2B_4O_7$ and $Na_2B_4O_7$ mineralise spinel formation from stoichiometric MgO and Al_2O_3 between 1000 and 1100 °C.[48] Mineralisation with both compounds is shown to be mediated by B-containing liquids which form glass on cooling. However, the liquid compositions depend on the type of mineraliser and temperature suggesting templated grain growth or dissolution–precipitation mechanisms operating; one dominating over the other under certain conditions. The mechanism of spinel mineralisation by $Na_2B_4O_7$ is illustrated in Fig. 10. $Na_2B_4O_7$ melts at 751 °C dissolving magnesia by 900 °C forming a Mg, Na borate liquid which facilitates spinel formation by templated growth on the alumina. All MgO is dissolved by 1000 °C but small corundum cores remain even after 3 h at 1100 °C even though at this temperature the mechanism is dissolution–precipitation. By 1100 °C the liquid is Mg,Na boroaluminate as alumina is also dissolving. Volatilisation of Na_2O and B_2O_3 is expected to reduce the volume of liquid at high temperatures.

$Na_2B_4O_7$-mineralized compositions thus show predominantly templated grain growth at 1000 °C which changes to dissolution-precipitation at 1100 °C. On the other hand $Li_2B_4O_7$-mineralized compositions show only dissolution-precipitation from 1000 °C once the $Li_2B_4O_7$ has melted (917 °C). $Li_2B_4O_7$ is a stronger mineraliser as spinel formation is complete with 3 wt% $Li_2B_4O_7$ at 1000 °C and with ≥1.5 wt% addition at 1100 °C, whereas $Na_2B_4O_7$-mineralised compositions retain some unreacted corundum at 1100 °C. $Li_2B_4O_7$ should be the favoured mineraliser in practical use.

Fig. 11 shows the coarse microstructural differences for the various mineralisers after 3 h at 1100 °C. With no mineraliser present the tuber-like spinel retains corundum cores, with 1.5 wt% B_2O_3 the spinel network is connected by slightly darker glass, with 1.5 wt% $Li_2B_4O_7$ a tuber-like spinel network is again present while with 1.5 wt% $Na_2B_4O_7$ extensive rim structures revealing corundum cores remain. The effect of the liquid composition on the microstructures is clear.

8. Concluding remarks

Five examples from the authors' own research into processing and use of ceramics have been used to illustrate the impact of liquid generation on the microstructures and thus, although not considered here, properties. It is clear that when and where the liquid forms and how it evolves with time, temperature, atmosphere and location is important. Each system highlights specific factors that influence the liquid and no doubt there are many more which must be considered before a thorough understanding of solid–liquid interactions in ceramic systems is achieved. What warrants further discussion is the volume of liquid present in the system. In slag attack of refractories a large volume of molten silicate slag is in direct contact with a porous solid refractory which also may contain liquid in its matrix system even before it is penetrated. The bulk slag composition is quite different from that penetrating and then reacting with the refractory and the formation of solid reaction products may protect the refractory from further attack. Denuding the penetrating (local) liquid from certain species will affect its composition and viscosity and careful design of the refractories microstructure can again lead to improved lining lives. Clay-derived ceramics at high temperature are up to 60 vol% liquid leading to highly heterogeneous microstructures with complex phase evolution on firing; the viscous matrix liquid hosting several microaggregate systems each reacting to form specific phase systems and each of which has differing liquid composition. For example, the liquid surrounding dissolving quartz is mostly silica, that hosting primary mullite is mostly aluminosilicate while that hosting secondary mullite is aluminosilicate enriched in alkalis. The composition and viscosity of this local liquid has a significant influence on the mullite morphology. Vitreous ceramic systems also reveal that atmosphere can have a large impact especially in silicate liquids containing elements with variable oxidation states such as Fe. Crystallisation of silicates which are completely liquid but which are effectively solid (glasses) reveals the importance of coupled crystallisation of several phases simultaneously or in sequence. They also highlight the effect of precipitation of each phase on the composition of the remaining liquid (glass) and hence its ability to form crystals. Large volumes of liquid host the key reactions during molten salt synthesis of solid ceramic powders with varying and controllable shapes and sizes. In solution-precipitation with two starting oxides both dissolve into the melt although often at different rates and the mixed oxide solid precipitates when its solubility limit in the melt is reached. More complex multi-oxide systems are worthy of study. In template synthesis one of the oxides is insoluble in the melt and provides a solid surface on which the other can deposit and react. Various processing variables including temperature, oxide source and salt/oxide ratio can be used to control the size and shape of the particles formed. The host melt viscosity is key to this control. Solution-precipitation and template mechanisms were also observed to operate on mineralisation of spinel formation in systems with much lower liquid levels than used in molten salt synthesis. Sometimes these processes were observed to compete with each other for spinel formation, temperature and time could be used to control which was dominant. The host liquid composition varied continuously as differing phases dissolve and precipitate. In the $Na_2B_4O_7$ mineralised system volatilisation of the Na (and B) altered the liquid composition and affected the mineralisation, a situation likely to be operative in many other examples.

Acknowledgement

It is with great pleasure that the lead author (WEL) acknowledges the great support of Prof. Sir Richard Brook throughout his academic career.

References

1. Lee, W. E. and Rainforth, W. M., *Ceramic Microstructures: Property Control by Processing*. Chapman and Hall, 1994.
2. Du, J. and Cormack, A. N., Molecular dynamics simulation of the structure and hydroxylation of silica glass surfaces. *J. Am. Ceram. Soc.*, 2005, **88**(9), 2532–2539.

3. Eustathopoulos, N., Nicholas, M. G. and Brevet, B., *Wettability at High Temperatures*. Pergamon, 1999.
4. Lee, W. E. and Zhang, S., Melt corrosion of oxide and oxide-carbon refractories. *Int. Mater. Rev.*, 1999, **44**(3), 77–105.
5. Lee, W. E., Argent, B. B. and Zhang, S., Complex phase equilibria in refractories design and use. *J. Am. Ceram. Soc.*, 2002, **85**(12), 2911–2918.
6. Clarke, D. R., On the equilibrium thickness of intergranular glass phases in ceramic materials. *J. Am. Ceram. Soc.*, 1987, **70**(1), 15–22.
7. Sato, Y., Yamamoto, T. and Ikuhara, Y., Atomic structures and electrical properties of ZnO grain boundaries. *J. Am. Ceram. Soc.*, 2007, **90**(2), 337–357.
8. Akbas, M. A., McCoy, M. A. and Lee, W. E., Microstructural evolution during pressureless sintering of lead lanthanum zirconate titanate ceramics with excess lead (II) oxide. *J. Am. Ceram. Soc.*, 1995, **78**(9), 2417–2424.
9. Hillers, M., Matzen, G., Veron, E., Dutreilh-Colas, M. and Douy, A., Application of *in situ* high temperature techniques to investigate the effect of B_2O_3 on the crystallization behavior of aluminosilicate E-glass. *J. Am. Ceram. Soc.*, 2007, **90**(3), 720–726.
10. Hasnain, I. A. and Donald, A. M., Microrheological characterisation of anisotropic materials. *Phys. Rev.*, 2006, **E73**(3) [Article No. 031901].
11. Korgul, P., Wilson, D. R. and Lee, W. E., Microstructural analysis of corroded alumina-spinel castable refractories. *J. Eur. Ceram. Soc.*, 1997, **17**, 77–84.
12. Goto, K., Argent, B. B. and Lee, W. E., Corrosion of MgO-$MgAl_2O_4$ spinel refractory bricks by calcium aluminosilicate slag. *J. Am. Ceram. Soc.*, 1997, **80**(2), 461–471.
13. Zhang, S., Rezaie, H. R., Sarpoolaky, H. and Lee, W. E., Alumina dissolution into silicate slag. *J. Am. Ceram. Soc.*, 2000, **83**(4), 897–903.
14. Sarpoolaky, H., Zhang, S. and Lee, W. E., Corrosion of high-alumina and near-stoichiometric spinels in iron-containing silicate slags. *J. Eur. Ceram. Soc.*, 2003, **23**(2), 293–300.
15. Zhang, S. and Lee, W. E., Use of phase diagrams in studies of refractories corrosion. *Int. Mater. Rev.*, 2000, **45**(2), 41–58.
16. Sarpoolaky, H., Zhang, S., Argent, B. B. and Lee, W. E., Influence of grain phase on slag corrosion of low cement castable refractories. *J. Am. Ceram. Soc.*, 2001, **84**(2), 426–434.
17. Chan, C.-F., Argent, B. B. and Lee, W. E., Influence of additives on slag resistance of Al_2O_3─SiO_2─SiC─C refractory bond phases under reducing atmosphere. *J. Am. Ceram. Soc.*, 1998, **81**(12), 3177–3188.
18. Lee, W. E., Zhang, S. and Sarpoolaky, H., Different types of *in situ* refractories. *Ceram. Trans.*, 2001, **125**, 245–252.
19. Rezaie, H., Rainforth, W. M. and Lee, W. E., Mullite evolution in ceramics derived from kaolinite, kaolinite with added α-alumina and sol–gel precursors. *Br. Ceram. Trans.*, 1997, **96**(5), 181–187.
20. Iqbal, Y. and Lee, W. E., Microstructural evolution in triaxial porcelain. *J. Am. Ceram. Soc.*, 2000, **83**(12), 3121–3127.
21. Iqbal, Y., Messer, P. F. and Lee, W. E., Microstructural evolution in bone china. *Br. Ceram. Trans.*, 2000, **99**(5), 193–199.
22. Souza, G. P., Rambaldi, E., Tucci, A., Esposito, L. and Lee, W. E., Microstructural variation in porcelain stoneware as a function of flux system. *J. Am. Ceram. Soc.*, 2004, **87**(10), 1959–1966.
23. Tarvornpanich, T., Souza, G. P. and Lee, W. E., Microstructural evolution on firing soda-lime-silica glass fluxed whitewares. *J. Am. Ceram. Soc.*, 2005, **88**(5), 1302–1308.
24. Lee, W. E., Souza, G. P., McConville, C. J., Tarvornpanich, T. and Iqbal, Y., Mullite formation in clays and clay-derived vitreous ceramics. *J. Eur. Ceram. Soc.*, 2008, **28**, 465–471.
25. Lee, W. E. and Iqbal, Y., Influence of mixing on mullite formation in porcelain. *J. Eur. Ceram. Soc.*, 2001, **21**(14), 2583–2586.
26. Souza, G. P., Messer, P. F. and Lee, W. E., Effect of varying quartz particle size and firing atmosphere on stoneware densification. *J. Am. Ceram. Soc.*, 2006, **89**(6), 1993–2002.
27. McConville, C. J., Lee, W. E. and Sharp, J. H., Microstructural evolution in fired kaolinite. *Br. Ceram. Trans.*, 1998, **97**(4), 162–168.
28. McConville, C. J. and Lee, W. E., Microstructural development on firing illite and smectite clays compared with that in kaolinite. *J. Am. Ceram. Soc.*, 2005, **88**(8), 2267–2276.
29. Tarvornpanich, T., Souza, G. P. and Lee, W. E., Microstructural evolution in clay-based ceramics I: single components and binary mixtures of clay, flux and quartz filler. submitted for publication.
30. Tarvornpanich, T., Souza, G. P. and Lee, W. E., Microstructural evolution in clay-based ceramics II: ternary and quaternary mixtures of clay, flux and quartz filler. submitted for publication.
31. Aksay, I. A. and Pask, J. A., Stable and metastable equilibria in the system SiO_2-Al_2O_3. *J. Am. Ceram. Soc.*, 1975, **58**(11–12), 507–512.
32. McCoy, M., Lee, W. E. and Heuer, A. H., Crystallization of MgO-Al_2O_3-SiO_2-ZrO_2 glasses. *J. Am. Ceram. Soc.*, 1986, **69**(3), 292–296.
33. Lee, W. E., Chen, M. and James, P. F., Crystallisation of celsian ($BaAl_2Si_2O_8$) glass. *J. Am. Ceram. Soc.*, 1995, **78**(8), 2180–2186.
34. Glendenning, M. and Lee, W. E., Microstructural development on crystallising hot pressed pellets of cordierite melt glass containing B_2O_3 and P_2O_5. *J. Am. Ceram. Soc.*, 1996, **79**(3), 705–713.
35. Jordery, S., Lee, W. E. and James, P. F., Crystallisation hierarchy of CaO-P_2O_5-SiO_2-Al_2O_3-TiO_2 glass ceramics. *J. Am. Ceram. Soc.*, 1998, **81**(9), 2237–2244.
36. Jais, U. S., Lee, W. E. and James, P. F., Crystallisation of barium osumilite glass. *J. Am. Ceram. Soc.*, 1999, **82**(11), 3200–3208.
37. Beall, G. H., Design and properties of glass-ceramics. *Annu. Rev. Mater. Sci.*, 1992, **22**, 91–119.
38. Beall, G. H., Glass-ceramics: recent developments and applications. In *Ceramic Transactions: Nucleation and Crystallization in Liquids and Glasses*, ed. M. C. Weinberg. The American Ceramic Society, Westerville, Ohio, 1993, pp. 241–266.
39. Lee, W. E., Arshad, S. E. and James, P. F., Importance of crystallisation hierarchies in microstructural evolution of silicate glass-ceramics. *J. Am. Ceram. Soc.*, 2007, **90**(3), 727–737.
40. Arshad, S. E., Comparing crystal evolution in model and commercial glass-ceramic systems. Ph.D. thesis. Department of Engineering Materials, University of Sheffield, 2005.
41. Hashimoto, S., Zhang, S., Lee, W. E. and Yamaguchi, A., $MgAl_2O_4$ spinel platelet production from α-Al_2O_3 platelet and $MgSO_4$ precursors. *J. Am. Ceram. Soc.*, 2003, **86**(11), 1959–1961.
42. Zhang, S., Jayaseelan, S. S., Bhattacharya, G. and Lee, W. E., Molten salt synthesis of magnesium aluminate ($MgAl_2O_4$) spinel powder. *J. Am. Ceram. Soc.*, 2006, **89**(5), 1724–1726.
43. Li, Z., Zhang, S. and Lee, W. E., Low temperature synthesis of $CaZrO_3$ powder from molten salts. *J. Am. Ceram. Soc.*, 2007, **90**(2), 364–368.
44. Li, Z., Zhang, S. and Lee, W. E., Molten salt synthesis of $LaAlO_3$ powder at low temperatures. *J. Eur. Ceram. Soc.*, 2007, **27**, 3201–3205.
45. Li, Z., Zhang, S. and Lee, W. E., Molten salt synthesis of zinc aluminate powder. *J. Eur. Ceram. Soc.*, 2007, **27**, 3407–3412.
46. Jayaseelan, D. D., Zhang, S., Hashimoto, S. and Lee, W. E., Template formation of magnesium aluminate (MgAl2O4) spinel microplatelets in molten salt. *J. Euro. Ceram. Soc.*, 2007, **27**, 4745–4749.
47. Lee, W. E., Zhang, S. and Karakus, M. N., Refractories: controlled microstructure composites for extreme environments. *J. Mater. Sci.*, 2004, **39**, 6675–6685.
48. Bhattacharya, G., Zhang, S., Smith, M. E., Jayaseelan, D. D. and Lee, W. E., Mineralizing magnesium aluminate spinel formation with B_2O_3. *J. Am. Ceram. Soc.*, 2006, **89**(10), 3034–3042.
49. Bhattacharya, G., Zhang, S., Jayaseelan, D. D. and Lee, W. E., Mineralizing effect of $Li_2B_4O_7$ and $Na_2B_4O_7$ on magnesium aluminate spinel formation. *J. Am. Ceram. Soc.*, 2007, **90**(1), 97–106.